Weak turbulence and structure evolution in N-body Hamiltonian systems with long-range force

Mickaël Antoni,[1,2,3,*] Yves Elskens,[3,†] and Caroline Sandoz[3]

[1]*Max-Planck-Institut für Physik Komplexer Systeme, Nöthnitzer Strasse 38, D-01187 Dresden, Germany*
[2]*INFM, Laboratorio FORUM, Università di Firenze, Largo Fermi, 2, I-50139 Firenze, Italy*
[3]*Equipe Turbulence Plasma de l'URA 773–UMR 6633, CNRS, Université de Provence, Centre de Saint-Jérôme,
Case 321, Avenue Escadrille Normandie-Niemen, F-13397 Marseille Cedex 20, France*

The dynamics of a family of one-dimensional spatially periodic systems of N classical particles interacting by a repulsive pair force is investigated. This force is the long-range part of the one-dimensional Coulomb interaction; the family includes the mean-field Hamiltonian rotator model. Initial conditions generating turbulent structures are considered. These structures are density holes in (x,v) space that produce a non-Gaussian probability distribution of fluctuations of the particle distribution function $f(x,v,t)$. These density holes appear in a velocity domain where $f(x,v)$ has large derivative $\partial_v f$ as predicted by the kinetic theory of clumps in plasmas. Their evolution is shown to be controlled by the motion of the particles in the (x,v) space domain swept by the separatrix associated with the longest-range coupling field components, which implies that their lifetime is proportional to the number N of particles. The relaxation time of the velocity distribution function of tagged particles in the system (for various initial conditions) is also shown to be quite insensitive to the presence of turbulent structures and to spatial scales smaller than the Debye length. [S1063-651X(98)08905-3]

PACS number(s): 05.45.+b, 64.60.Cn, 52.20.Dq, 52.35.Fp

I. MOTIVATIONS

Systems of many particles interacting via two-body long-range forces have peculiar equilibrium and nonequilibrium statistical mechanics [1,2]. The Coulomb system, which has been thoroughly investigated, combines the difficulties of long-range interaction with a short-range divergence — or, in one dimension, with a discontinuity in the electric field. Recent numerical simulations [3–6] and theoretical arguments [7–10] indicate that the characteristics of Coulombian plasma turbulence are shared by a family of systems in which only the smooth, long-range part of the Coulomb interaction is considered. Such models are discussed in solid state and nuclear physics (see, e.g., Ref. [11] and references therein).

A proper understanding of the analogy and differences between the systems with long-range pair interactions requires more than a discussion of their equilibrium statistical mechanics. The aim of the present paper is to show how systems with long-range interactions behave similarly to the Coulomb one in the evolution of their (x,v)-space densities. Indeed non-wave-like fluctuations (phase-space granulations) are an important element of Vlasov turbulence in plasma physics (see, e.g., Refs. [13–17] and references therein, and Ref. [18] for a review). These granulations (''clumps'' and ''holes'') are domains with an excess or a depletion of particles, on a length scale comparable with the Debye length and a velocity range of the order of a fraction of the thermal velocity. They last for long times compared with the local rate of separation of trajectories [19] and may be presented as nonequilibrium, nonlinear, robust self-organized structures [18,20]. Therefore, while the theoretical basis on which they were analyzed is kinetic theory, they should be considered as manifestations of the finiteness of the number of particles in the system, but the limitations in computer power precluded numerical investigations along this line so far.

It has been known for decades that the behavior of the (x,v) space density of particles interacting by a long range force like Coulomb's is described in the limit $N\to\infty$ by the Vlasov equation. Granularity effects have been computed through the Balescu-Lenard equation. However, the typical form of rigorous estimates on the growth of discrepancies between kinetic-theoretical evolution and finite-N evolution is exponential in time for smooth pair interaction [21,22], and the Vlasov-Poisson system in one space dimension with smooth initial conditions is able to generate in finite time singularities in the form of ''particlelike'' (Dirac) concentrations [23]. This prompts for a more direct study of such finite N effects. The present paper aims to show that phase space $[(x,v)$ space] granulations also appear when the interparticle interaction is a smooth long-range one. In the latter case, we take advantage of the development of adapted numerical codes.

In Sec. II we present our family of models (with parameter s), in which the interaction reduces to the Coulomb form in the limit $s\to\infty$. The case $s=1$, or ''mean field XY'' or rotator model, was introduced by Antoni and Ruffo [3,12]. Larger values of s correspond to a Coulomb interaction truncated to its s Fourier components with smallest wave number (i.e., longest range). Codes and initial conditions are described in Sec. III.

In Sec. IV we characterize the relaxation of the distribution of ''tagged'' particles (i.e., test particles in the system) to the ambient distribution, starting from an equilibrium state as well as from a nonequilibrium initial condition. Turbulent structures generated by our simulations are characterized in

*Electronic address: antoni@jollyjumper.mpipks-dresden.mpg.de

†Electronic address: elskens@newsup.univ-mrs.fr
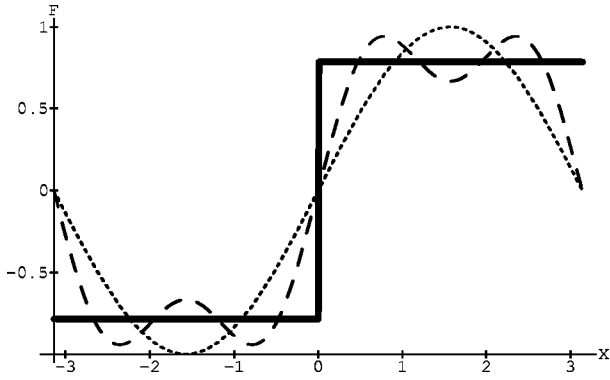
FIG. 1. Pair interaction force $F(x)$ for Lenard-Prager plasma ($s'=\infty$: full line) and for truncations to first Fourier components ($s'=1$: dots, $s'=3$: dashed line), with $q=\epsilon_0=1$, $L=2\pi$.

Sec. V, where we compare the true one-dimensional (1D) N-body dynamics of Coulomb interacting particles with the kinetic approach [16] and with N-body dynamics of finite-s interactions. The relaxation of the fields to equilibrium, which occurs on longer time scales than the turbulent motion of Sec. V, is investigated in Sec. VI, and we propose a dynamical description that may complement the kinetic approach. The interaction between structures generated by similar initial conditions is presented in Sec. VII. Conclusions are summarized in Sec. VIII.

II. HAMILTONIAN ROTATOR MODEL

Our system of N identical classical particles is described by the Hamiltonian

$$H=K+V=\sum_{r=1}^{N}\frac{p_r^2}{2m}+\frac{q^2}{2N}\sum_{n=1}^{s'}\sum_{l,r=1}^{N}V_n\cos[k_n(x_r-x_l)],$$
(1)

where $x_r\in\mathbb{R}/L$ is the position of particle r (with mass m and charge q) on the interval of length L with periodic boundary conditions (i.e., the circle S_L), p_r is its conjugate momentum, and $k_n=2\pi n/L$. The Fourier coefficients V_n of the potential are positive with finite sum [24].

We are especially interested in the family

$$V_n=n^{-2}K',\quad 1\leq n\leq s',\quad n\text{ odd}$$
(2)

and denote by $s=(s'+1)/2$ the number of nonvanishing coefficients. In the limit $s\to+\infty$ with $K'=L/(\pi^2\epsilon_0)>0$, model (1) with coefficients (2) defines a one-dimensional Coulombian system [24]. The field generated by a particle at x_j reads $(K'q/N)\sum_{n'=1}^{\infty}\sin[k_{2n'-1}(x-x_j)]=(\pi K'q/4N)\mathrm{sgn}\sin[2\pi(x-x_j)/L]$, which is constant on both sides of the particle and has a jump at location $x_j+L/2$. Calling our particles electrons, this jump may be interpreted as due to a positron at this opposite location. This model, equivalent to the model investigated by Lenard and Prager [25,26], may thus be considered as a two-species plasma model on the semicircle of length $L/2$, with boundary condition such that when a particle exits at 0 its antiparticle enters at $L/2$ with the same velocity (and conversely). Figure 1 displays the

field for this interaction and its truncation to the first Fourier components (finite s rotator models).

Hamiltonian (1) yields the equations of motion

$$m\ddot{x}_j=N^{-1}\sum_{n=1}^{s'}\sum_{r=1}^{N}k_nV_nq^2\sin k_n(x_j-x_r).$$
(3)

The nth-order total field component $\mathbf{S}_n$, its amplitude S_n, and its phase ϕ_n are defined as

$$\mathbf{S}_n=\left(N^{-1}\sum_{j=1}^{N}q\cos k_nx_j,N^{-1}\sum_{j=1}^{N}q\sin k_nx_j\right)$$
$$=(S_n\cos\phi_n,S_n\sin\phi_n)$$
(4)

with $-\pi<\phi_n\leq\pi$. With no loss of generality, letting $m=1$, $q=1$, and introducing the new coordinate $X_i=2\pi x_i/L+\pi\bmod(2\pi)$, the force in Eq. (3) can be reexpressed as a sum of s' terms:

$$\ddot{X}_i=-\frac{2\pi}{L}\sum_{n=1}^{s'}k_nV_nS_n\sin(nX_i-\phi_n),$$
(5)

where both S_n and ϕ_n depend on time [cf. Eqs. (4)]. The N-body motion thus reduces to a single particle problem in the self-consistent fields (S_n,ϕ_n) with $n=1,2,\ldots,s'$.

Expression (4) implies that the two components of $\mathbf{S}_n$ are proportional to the nth discrete Fourier coefficients of the spatial distribution. Hence, the time evolution of the collective quantities $\phi_n(t)$ and $S_n(t)$ will characterize the dynamics occurring on spatial scale L/n. In a previous work [24] we considered the equilibrium statistical mechanical properties of this model. This system undergoes no phase transition if all coupling constants V_n are non-negative (i.e., if all couplings act repulsively). The Gibbs canonical distribution of fields $\mathbf{S}_n$ at temperature $T=\langle p_r^2\rangle$ for $N\to\infty$ is Gaussian, isotropic, with independent components $\mathbf{S}_n$ having average square modulus

$$\langle S_n^2\rangle=N^{-1}\frac{2T}{2T+V_n}.$$
(6)

The equilibrium correlation function, i.e., the density at distance y from a test particle, is given by

$$C(y)=\langle\delta(x_1-x_2-y)\rangle=\frac{1}{L}+\frac{c(y)}{N-1}$$
$$=\frac{1}{L}+\frac{2}{L(N-1)}\sum_{n=1}^{\infty}C_n\cos(k_ny)$$
(7)

with $C_n=N\langle|\mathbf{S}_n|^2\rangle-1=-V_n/(2T+V_n)$. In the (Lenard-Prager) 1D Coulomb case, the equilibrium correlation function decays exponentially, with the Debye characteristic length

$$\lambda_D=k_D^{-1}=\left(\frac{L\epsilon_0T}{2q^2}\right)^{1/2}=\frac{L}{\pi}\left(\frac{T}{2K'}\right)^{1/2}.$$
(8)

The nearness of the finite-N system to the ''kinetic limit'' ($N\to+\infty$) is measured by the mean number of particles per

Debye length $N_D = N\lambda_D/L$, or by the grain parameter N_D^{-1}. The physical characteristic time on macroscopic scales is the reciprocal of the plasma pulsation

$$\omega_{\text{pl}} = k_D v_{\text{th}} \tag{9}$$

and the characteristic velocity is $v_{\text{th}} = \sqrt{2H/N}$. We use these expressions for the cases $s < \infty$ as well as for the 1D Coulomb case to facilitate comparisons. Note that k_D, v_{th}, and ω_{pl} are finite in the limit $N \to +\infty$ if one keeps the mean energy per particle H/N or temperature T fixed.

Because the particle interaction is repulsive, the total potential energy

$$V = H - K = \frac{N}{2} \sum_{n=1}^{s'} V_n S_n^2 \tag{10}$$

is $O(N^{-1})$ times smaller than the total kinetic energy in equilibrium states. Initial conditions may have larger potential energy, but the system relaxes to values of S_n of the order of Eq. (6): nonequilibrium situations with S_n in such a range are called *weakly turbulent* by analogy with the Coulombian plasma case [27]. Thus the instantaneous rms velocity (or thermal velocity) $\langle p_r^2 \rangle^{1/2} = (2H/N - \Sigma_n |\mathbf{S}_n|^2)^{1/2} = v_{\text{th}} + O(N^{-1})$ in such regimes, and $\omega_{\text{pl}} = \sqrt{K'/2}$.

The purpose of the present paper is to characterize nonequilibrium behaviors of our systems such as relaxation to thermal equilibrium. For the 1D Coulombian (charged sheets) model, we shall compare the results of N-body dynamics with the more common kinetic theory. For the rotator model ($s = 1$), our work is the first investigation of its weakly turbulent regimes; the low temperature regime has already been considered by Antoni and Ruffo [3], who observed the formation of clusters in spite of the interparticle repulsion. The high temperature behavior of the $s = 1$ rotator model is also investigated currently with focus on its dynamical instabilities [28].

III. CODES AND INITIAL CONDITIONS

To integrate Eq. (5) with s finite, we use a second order symplectic scheme (leap-frog) [3], developed in analogy with the code used successfully for modeling the interaction of N particles with s waves [29]. Since the force on each particle depends only on the mean fields $\mathbf{S}_n$, the algorithm requires $O(Ns)$ CPU time instead of $O(N^2 s)$. For reasonable values of s we can consider values of N larger than 10^4. This numerical scheme is easily vectorized, as one computes successively the field components $\mathbf{S}_n$ from all particle positions, and then one advances the particles independently of each other using only their own position and velocity and the instantaneous fields.

From the numerical analysis viewpoint, our truncation of the binary interaction is a particular type of "mollification" regularizing the dynamics [21,23]. Then, for $s < \infty$, the limit $N \to \infty$ leads to a regular kinetic limit with a unique solution for all times to the initial value problem [21,22].

In the limit $s \to +\infty$, the particles behave like parallel charged sheets that cross each other smoothly. Between two crossings, the force on a particle is constant. The dynamics is thus locally integrable in time. To integrate model (1) in this
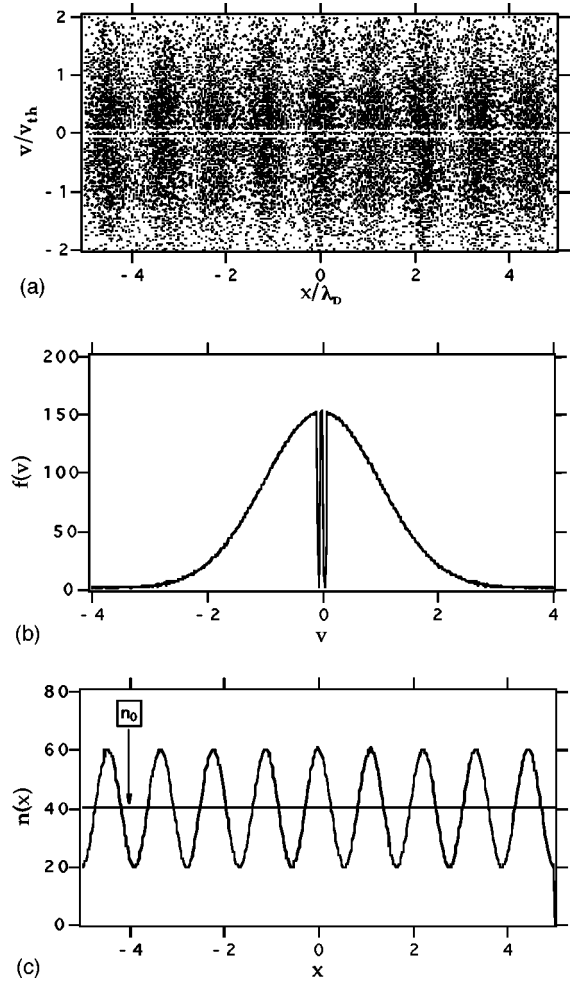

FIG. 2. Typical initial condition with $N = 20\,000$ particles, $\lambda_D = L/10$. Spatial density modulated at wavelength $L/9$ and Maxwell velocity distribution function with gaps at $0.03 < |v/v_{\text{th}}| < 0.08$. (a) (x,v) space plot (one dot per particle). (b) Histogram of number of particles per cell in v space (plot restricted to $-2 < |v/v_{\text{th}}| < 2$). (c) Histogram of number of particles per cell in x space.

case, we use an "exact" integration scheme [9,10,30–33,5] in which the only numerical errors are caused by the truncation of real numbers to the machine accuracy. This scheme is also $O(N)$.

To allow direct comparison with earlier work on kinetic plasma turbulence, we use initial conditions similar to that considered in Ref. [16], such as plotted on Fig. 2(a) in the (x,v) plane (for $N = 20\,000$). The (reference) equilibrium distribution is uniform in space and Maxwellian in velocities. The dimensionless control parameter for this equilibrium is the ratio of the Debye length λ_D to the system length $L = 2\pi$, or equivalently the ratio of thermal velocity v_{th} to $L\omega_{\text{pl}}$; we set $\omega_{\text{pl}} = 1$ with no loss of generality in our numerical experiments. The thermal velocity is given the value $v_{\text{th}} = 2\pi/10$ to fit 10 Debye lengths on the circle (normalized to 2π).

The initial perturbation is twofold. The velocity distribution [Fig. 2(b)] is a Maxwell distribution from which we remove all the particles in two narrow symmetric velocity domains (here $0.03 \leq |v/v_{\text{th}}| \leq 0.08$). These gaps generate (in the kinetic approach) turbulence in their neighborhood, leading to the formation of "hole"-like coherent structures [16].
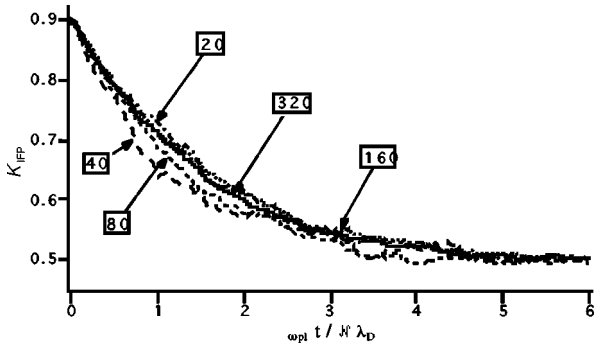
FIG. 3. Relaxation of the fraction of kinetic energy shared by initially fast particles vs time, for the 1D Coulombian case ($L = 2\pi = 10\lambda_D$). Time axis rescaled by $N_D\omega_{pl}^{-1}$. Number of particles per Debye length $N_D = N/10 = 20,40,80,160,320$.

The spatial distribution of the particles is modulated with a period close to the Debye length λ_D to excite structures similarly (in the plasma context, Debye-scale density modulations would be short lived due to Landau damping [34]). Figure 2(c) displays the spatial density corresponding to Fig. 2(a), i.e., $n(x) = n_0 + n_1 \cos(2\pi x/\lambda)$, with $\lambda = 10\lambda_D/9$, $n_0 = N/L$, $n_1 = 0.5n_0$.

Numerical simulations starting from uniform initial spatial distributions were also performed.

IV. RELAXATION OF TAGGED PARTICLES DISTRIBUTION

Let us first estimate the typical time needed by *tagged* particles to get mixed among the other particles, starting from an equilibrium distribution. Given an initial Maxwellian (or nearly so) distribution of velocities, and a uniform spatial density, we distinguish two families of particles [7,3,5]: the $N/2$ initially fast particles (IFP) and the $N/2$ initially slow particles (ISP). These families are well defined regardless of whether a turbulent structure or a density modulation are present or not. Denote by

$$K_{\text{IFP}}(t) = \frac{1}{K(t)} \sum_{r \in \text{IFP}} \frac{p_r^2}{2}, \qquad (11)$$

the fraction of the total kinetic energy $K(t)$ shared by the initially fast particles. Its relaxation time measures the typical time needed by a particle to undergo a significant velocity variation. As $t \to +\infty$, $K_{\text{IFP}}(t)$ relaxes to 1/2, and when $K_{\text{IFP}}(t) \approx 1/2$, one can consider that the particles have lost memory of their initial velocity. Initially, we have $K_{\text{IFP}}(t) \approx 0.9$. Figure 3 displays $K_{\text{IFP}}(t)$ as a function of time for various numbers of particles for the 1D Coulombian case [7].

The rotator models with finite s behave similarly, and we plot on Fig. 4 the time $\tau_r(N,s)/N$ needed by $K_{\text{IFP}}(t)$ to reach the value 0.8. As our diagnostic is easily applied to nonequilibrium initial distributions, Fig. 4 displays not only data obtained from a spatially uniform initial condition (circles) but also data evolved from the initial condition of Fig. 2 (black markers and crosses).

Like the time scales of Sec. VI below, the characteristic times obtained here are proportional to the total number of
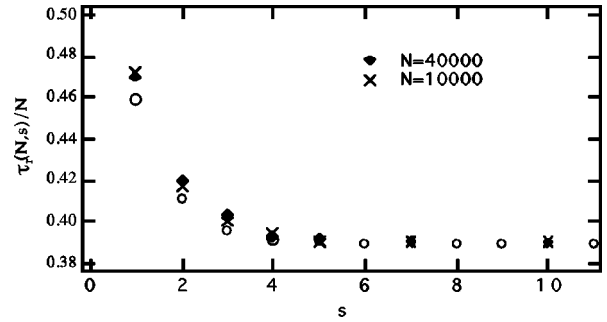

FIG. 4. Relaxation time of the tagged particles total kinetic energy vs number s of nonzero coefficients in the potential. Initial conditions are spatially uniform (open circles, $N = 10\,000$) and modulated spatially (black markers for $N = 40\,000$, crosses for $N = 10\,000$).

particles N. We shall further discuss the reason for this scaling in Sec. VI. These results complement results of Refs. [32,33], which made a similar observation for the 1D Coulombian system.

The s dependence in Fig. 4 shows that the relaxation time scale τ_r of the velocity distribution function is not sensitive to the interaction on spatial scales smaller than λ_D. Besides, the closeness of the time scales for the same s and different initial conditions implies that the tagged particle relaxation time does not depend significantly on the presence of turbulent structures of Debye scale as those observed in the next section.

V. PHASE SPACE DENSITY HOLES

Now we turn to nonequilibrium structures supported by the dynamics. Following kinetic theory arguments for the Vlasov-Poisson integrodifferential system, Berman, Tetreault, and Dupree [16] find that weak plasma turbulence generates depletions rather than density excess in (x,v) space, and their simulations confirm these predictions. However, their simulation method uses particle-in-cell codes, which automatically smooth the distribution functions, and one is interested here in small scale structures, with a size close to grid mesh scales. In this section we first compare the structures generated by the microscopic N-body dynamics of the 1D Coulomb system with those obtained from the Vlasov-Poisson system in (x,v) space. We shall see that the formal difference between the two models on scales smaller than the Debye scale does not lead to different types of structures. Then we compare the Coulomb interaction, with all its Fourier components, to the ''truncated'' interaction, with only the longest-range Fourier component, i.e., to the rotator model with $s = 1$. We end this section by considering the effect of more Fourier components in the interaction.

A. The Coulombian model

Among the diagnostics used by Berman, Tetreault, and Dupree [16], (x,v)-space plots provide the most direct evidence for (x,v)-space granulations. Figure 5 displays a sequence of snapshots at various times for the 1D Coulombian system ($s = +\infty$) of $N = 20\,000$ particles. The velocity range displayed is limited to $|v/v_{\text{th}}| \lesssim 0.8$ where the structures actually evolve. The density hole observed near $x/\lambda_D \approx -1$
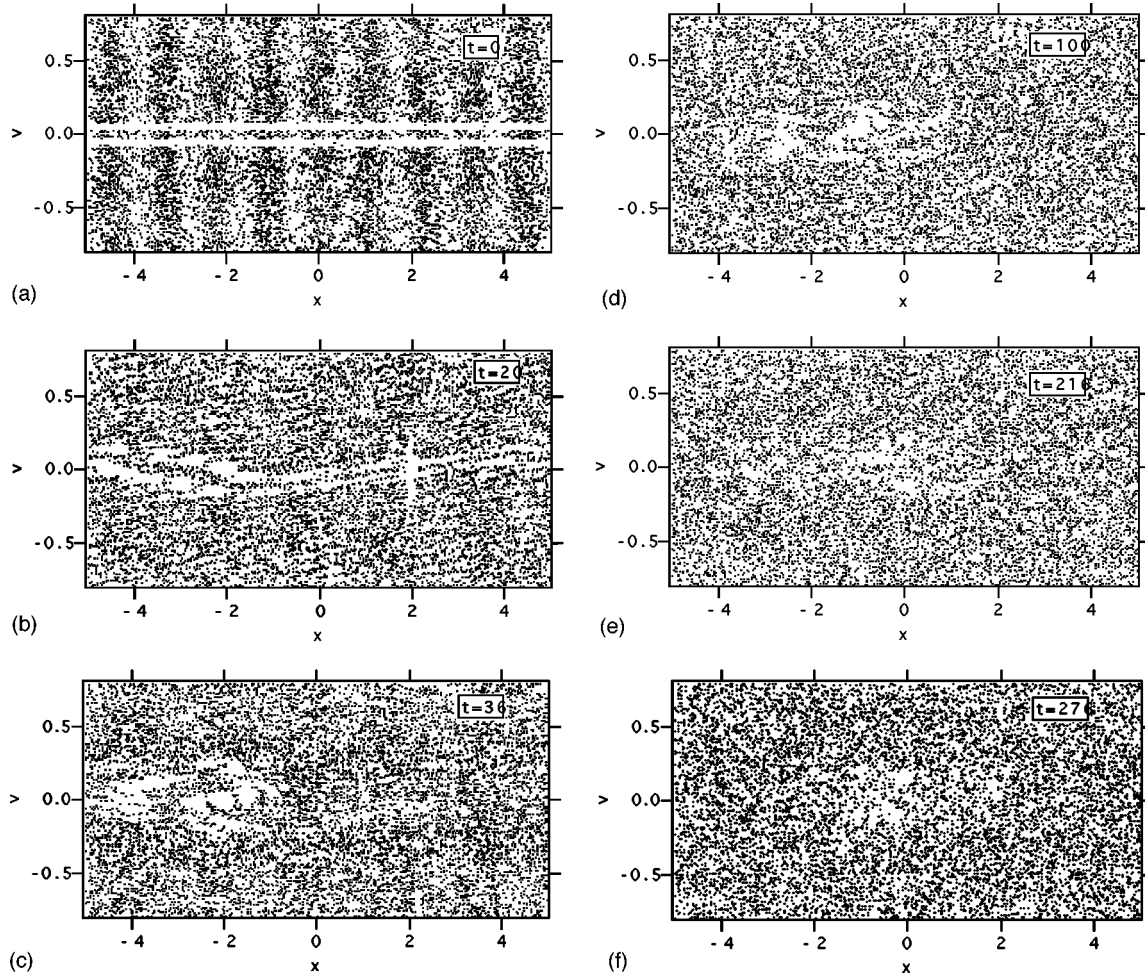
FIG. 5. (x,v) space for 1D Coulombian model ($s \to \infty$, or charged sheets) at successive times, starting from initial condition of Fig. 2.

moves slowly to the right and appears as a depletion in the space-averaged velocity distribution function.

This hole propagates at a characteristic velocity of the order of $0.1v_{th}$, i.e., in the velocity range in which the velocity distribution function initially has a steep derivative $\partial_v f$ (actually f initially has a gap so that $\partial_v f = \infty$ formally), in agreement with kinetic theoretical predictions [16].

A second, less visual, but robust, indication for granulations is obtained from a statistical test on the relative fluctuations δf of the population in (x,v) cells. For an equilibrium state, and for large scale perturbations as due to Langmuir modes (or their finite-s analogs), the number $A(x_0,v_0)$ of particles in a cell ($|x-x_0| \leqslant \Delta x/2$, $|v-v_0| \leqslant \Delta v/2$) is a Poisson random variable with expectation $A_{eq}(x_0,v_0) = f_{eq}(x_0,v_0)N\Delta x \Delta v$. Thus the relative fluctuation

$$\delta f(x_0,v_0) = A(x_0,v_0)/A_{eq}(x_0,v_0) - 1 \qquad (12)$$

is a random variable with vanishing expectation in equilibrium states. It is clear that $\delta f(x_0,v_0) \geqslant -1$ and that $\langle A_{eq}(x_0,v_0)\delta f(x_0,v_0)\rangle = 0$ for any state of the system. Moreover, for an equilibrium state, the distribution of relative fluctuations is expected to be nearly Gaussian [16].

We divide the range $|v| \leqslant v_{th}$ in 300 cells with sizes $\Delta x = \lambda_D/2$ by $\Delta v = v_{th}/15$. At equilibrium, there are $A_{eq} \approx 50$

particles in such a cell, which is large enough to yield significant statistics. We plot in Fig. 6 the distribution of δf for these cells at time $t = 216\omega_{pl}^{-1}$. This plot has an average $\langle \delta f \rangle = -0.2$ and a standard deviation $(\langle \delta f^2 \rangle - \langle \delta f \rangle^2)^{1/2} = 0.14$, indicating that the cells are depleted rather than overpopulated.

These diagnostics confirm the formation and evolution of holes in microscopic dynamics of the Coulombian model, showing that these structures appear in the same manner as in the kinetic plasma model. Correlation functions and bior-
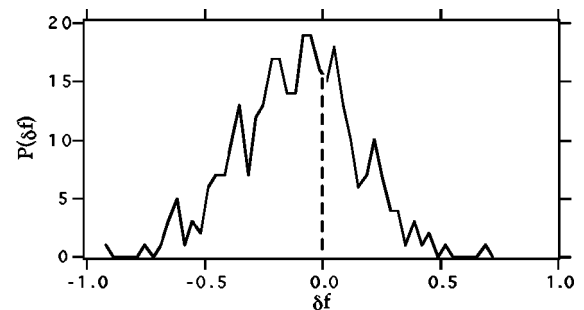

FIG. 6. Distribution of relative fluctuations of (x,v)-space density in range $|v| \leqslant v_{th}$ in the presence of hole structure, for 1D Coulomb system of Fig. 5. Ordinates in arbitrary units.
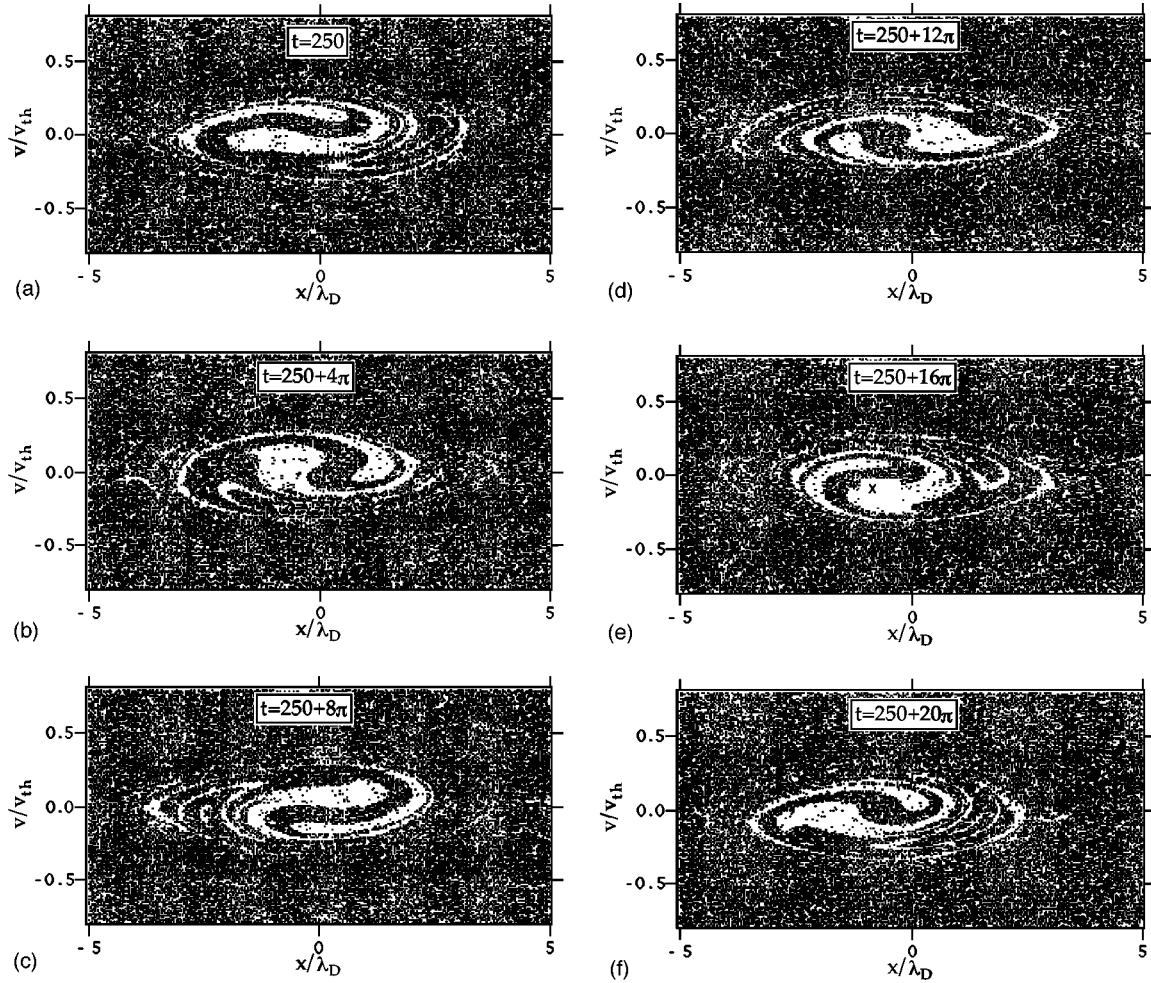
FIG. 7. (x,v) space for rotator model $(s=1)$, starting from initial condition of Fig. 2.

thogonal decomposition of the distribution function [5,6] lead to the same conclusion.

B. The rotator model

For $s=1$ with $L=2\pi$, equation of motion (5) reduces to the pendulum equation

$$\ddot{x}_r = K'S_1 \sin(x_r - \phi_1), \tag{13}$$

where intensity S_1 and phase ϕ_1 depend on all particles positions through Eq. (4). The interaction is ''only long range'' as the field $\mathbf{S}_1$ has wavelength 2π on the circle [3]. The time evolution of a system of $N=80\,000$ particles, starting from the initial condition of Fig. 2, is similar to the evolution of the Coulombian system. However, the absence of short-range components in the force (13) gives a smoother shape to the density hole as shown on Fig. 7. The (x,v)-space density relative fluctuations, displayed in Fig. 8, are similar to those of the previous section.

C. The modulated rotator interaction

For $s=2$ $(s'=3)$ with coefficients (2) a system of $N=80\,000$ particles evolves from the initial condition of Fig. 2 to the same type of structures as for $s=1$ and $s\rightarrow\infty$. Figure 9 displays an (x,v)-space picture at $t=250\omega_{pl}^{-1}$, and Fig. 10

shows the distribution of relative fluctuations δf. Similar results [5] were obtained for larger s.

The similarity between the structures observed for $s=1$, $s=2$, and larger s is easily explained by the fact that, according to Eq. (6), thermal equilibrium values of S_n are close to each other, so that coefficients (2) imply $k_n V_n S_n \sim n^{-1}$, and the long-range components are thus dominant in Eq. (5) in weak turbulence regimes.

VI. RELAXATION OF FIELDS TO EQUILIBRIUM

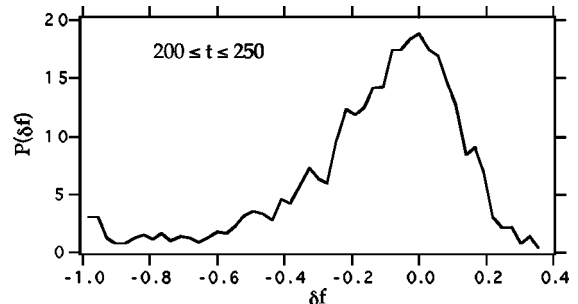The weakly turbulent structures of Sec. V characterize the behavior of particles in (x,v) space on ''microscopic''

FIG. 8. Distribution of relative fluctuations of (x,v)-space density in range $|v| \lesssim v_{th}$ in the presence of hole structure, for rotator system of Fig. 7. Ordinates in arbitrary units.
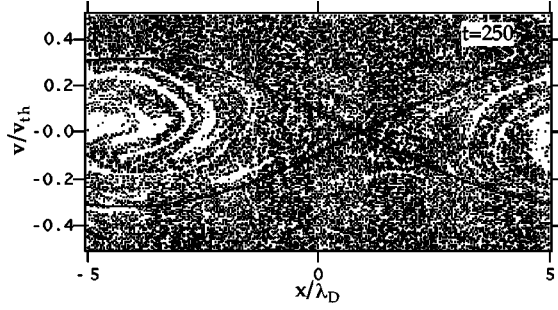
FIG. 9. (x,v)-space distribution of particles at $t=250\omega^{-1}$ for modulated $(s=2, s'=3)$ rotator system, evolved from initial condition of Fig. 2. Solid lines indicate the instantaneous separatrix of the resonance associated to S_1 of Sec. V B and Sec. VI B.

scales. The formation of these structures was triggered by perturbations of the initial distribution of particles, but the diagnostics of Sec. V were instantaneous. Now we consider ''macroscopic'' time scales, over which the fields S_n decay from nonequilibrium values to values of thermal magnitude.

A. Characteristic time scales

As the system dynamics is dominated by the (longest-range) field S_1, i.e., the first Fourier component of the inter-action field, we monitor its evolution to describe the approach to weakly turbulent quasistationary behavior, starting from modulated initial conditions. Figure 11 displays a typical evolution (for $s=2$, $N=80\,000$) of the amplitude S_1, of the phase ϕ_1, and of the phase velocity $d\phi_1/dt$. The initial condition is modulated so that $S_1(0)$ is a few times the thermal equilibrium value (6). The amplitude decays regularly and the phase velocity varies slowly over an interval $0<t<\tau_v$. At time τ_v, the amplitude reaches the equilibrium level (6) and the phase velocity gets dominated by noise.

For the same initial condition, with different values of s and N, the evolution of S_1 looks similar. Results summarized in Fig. 12 show that the time scale $\tau_v(N,s)$ is proportional to N. The dominance of the small-wave-number components appears in the fact that τ_v/N rapidly approaches its asymptotic value for increasing s.

The proportionality of τ_v to N may be explained for the plasma case as follows. Increasing the number of particles in the system makes the ''discrete distribution function'' $f_N(x,v,t)=N^{-1}\Sigma_r\delta(x-x_r(t))\delta(v-v_r(t))$ closer to a
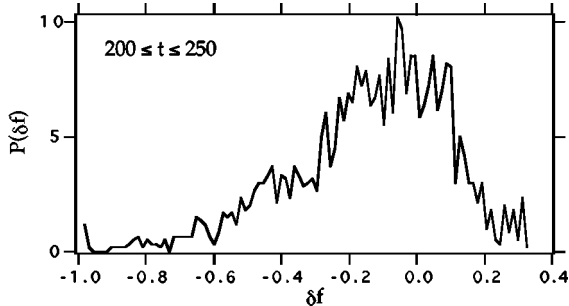

FIG. 10. Distribution of relative fluctuations of (x,v)-space density in range $|v|\lesssim v_{\text{th}}$ in the presence of hole structure, for modulated $(s=2, s'=3)$ rotator system of Fig. 9. Ordinates in arbitrary units.
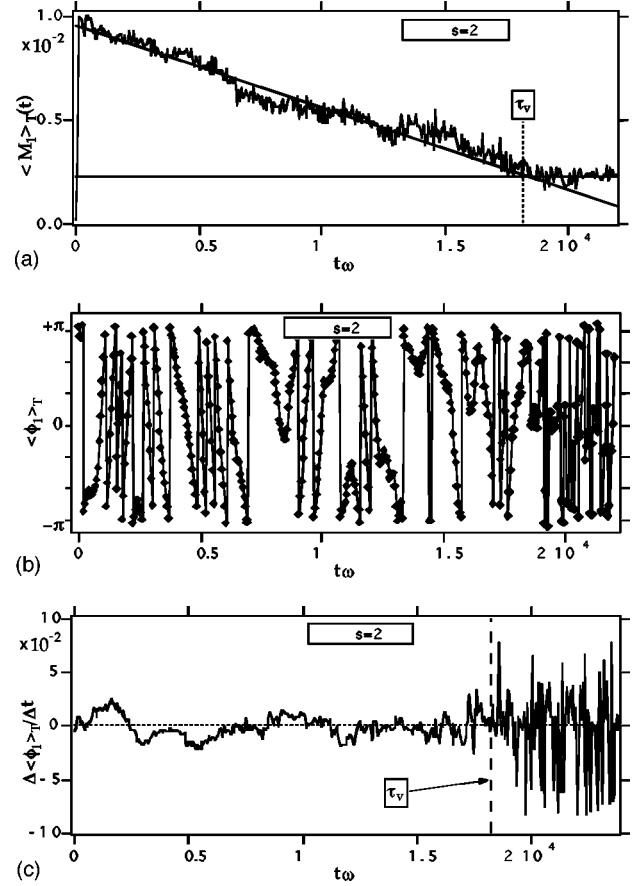

FIG. 11. Evolution of (a) amplitude S_1, (b) phase ϕ_1 modulo 2π and (c) phase velocity $d\phi_1/dt$ from a moderate initial modulation in the rotator system ($s=2$, $N=80\,000$).

smooth distribution function, which evolves following kinetic theory. The factor N^{-1} in the coupling term in Eq. (1) ensures that the macroscopic time scale ω_{pl}^{-1} (which governs hydrodynamiclike behavior of the Langmuir modes) is independent of N, but here we consider microscopic (''molecular dynamics'') evolution. In the plasma case, it has been shown that the distribution function relaxes on a time scale proportional to N because ''binary interactions'' must preserve energy and momentum (hence they cannot modify the distribution function as all particles have equal mass): the distribution function can relax only as a result of ''three-body interactions,'' for which the coupling is N^{-1} times weaker than the ''two-body coupling.''

Our results show that the truncated interaction behaves in the same way as the full Coulombian interaction, and that the time scales of the latter are reproduced already with a small number of Fourier components.

B. Particle motion and field evolution for $s=1$

Let us now describe the microscopic dynamics underlying the relaxation. We first consider the simple rotator case $s=1$. Then $k_1=1$ with $L=2\pi$, and $V_1=K'$. Equation (13) shows that any particle r moves in a pendulumlike field. We associate to this motion a *forced* Hamiltonian dynamics, generated by $e_r:=w_r^2/2+K'S_1\cos y_r$, where we treat S_1 as a time-dependent external parameter (i.e., we neglect the fact that particle r contributes to the evolution of S_1). Here y_r:
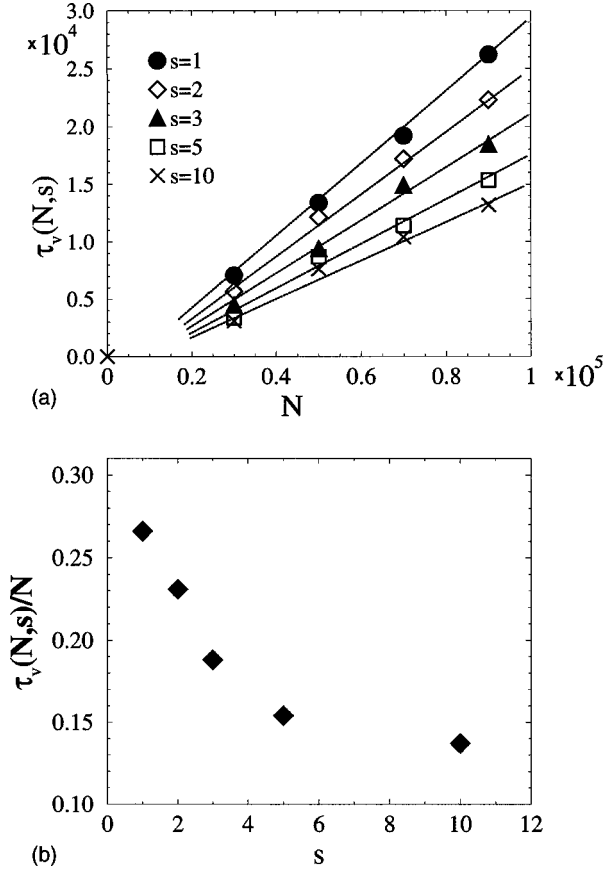
FIG. 12. (a) Lifetime $\tau_v(s,N)$ of turbulent structure vs number of particles for various values of s. (b) Normalized lifetime τ_v/N vs number s of Fourier components in the interaction.

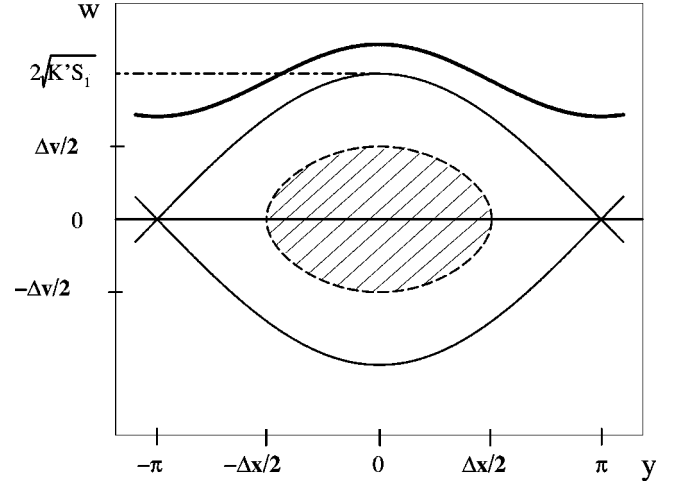

FIG. 13. Sketch of resonance in (y,w) plane associated to the effective one-particle reduced Hamiltonian $w_r^2/2+K'S_1\cos y_r$ with $L=2\pi$, $\phi_1=0$, $\dot{\phi}_1=0$. Resonance half-width is $2(K'S_1)^{1/2}$. Thin solid line is the instantaneous separatrix (two branches). Thick solid line is a typical particle orbit with $e>0$. Dotted line is a typical particle orbit near hole boundary. The field S_1 is generated self-consistently by a depletion of particles in the center of its resonance (typically inside shaded domain). The hole is centered on $(0,0)$ with characteristic size $(\Delta x,\Delta v)$. Compare with Figs. 7 and 9.

$=x_r-\phi_1$ and $w_r:=p_r-\dot{\phi}_1$ are conjugate variables in the co-moving frame of the resonance (obtained from x_r and p_r through a Galileo transformation). Thus particle r may be trapped or untrapped in the ''resonance'' generated by the density structure. This resonance is centered on ϕ_1, with instantaneous velocity $\dot{\phi}_1=d\phi_1/dt$, and its half width is $2\sqrt{K'S_1}$. The bouncing period for trapped particle motion is $2\pi/\omega_{\text{trap}}=2\pi(K'S_1)^{-1/2}$, and the exponential rate of divergence of trajectories at the structure's saddle point is $(K'S_1)^{1/2}$.

The self-consistent relation of the resonance with the hole it traps [15] is sketched in Fig. 13. First note that the dynamics of the resonance depends on all particles (contributing equally to S_1 with the same charge q), but that particles with velocity near $d\phi_1/dt$ play a dominant role as they are nearly fixed in the resonance frame. Particles moving with respect to the resonance generate an oscillating contribution that averages away to first approximation [10]. Thus we discuss only particles with $w\approx0$. If there is a depletion near a position x_h, the repulsive coupling ensures that the resonance will be centered near x_h (i.e., $\phi_1\approx x_h$) and the saddle will be near $x_h+L/2\,(\text{mod }L)$. As the particles follow constant energy e lines in the (y,w) plane, particles on the boundary of the hole move on closed, ellipselike orbits surrounding the hole. In the kinetic limit ($N\to\infty$), with Coulomb interaction ($s\to\infty$), such phase space pictures are characteristic of the Bernstein-Greene-Kruskal (BGK) modes of plasmas [38],

which are exact solutions of the kinetic Vlasov-Poisson system.

However, with a finite number of particles, BGK modes are perturbed. The slow drift in $\phi_1(t)$, i.e., global motion of the turbulent structures on the circle, is not a constant-velocity drift. To understand this motion we distinguish the trapped particles (TP) having energy $e_r<K'S_1$ from the untrapped ones (UP) with $e_r\geq K'S_1$. Denote by $\bar{p}_{\text{TP}}$ ($\bar{p}_{\text{UP}}$) the momentum of (un)trapped particles, which may be averaged over one (approximate) period of the (un)trapped motion. Then $\bar{p}_{\text{TP}}=\dot{\phi}_1$ as a trapped particle moves on the average at the same velocity as its trapping structure. Also, as S_1 is small, the momentum of an untrapped particle is almost constant: only particles with $e_r=O(K'S_1)$ have a motion sensitive to the field S_1, whereas for particles with $e_r\gg K'S_1$ the acceleration due to S_1 is averaged off.

Now recall that the field S_1 is generated by the distribution of particles. Statistical fluctuations induce $O(N^{-1/2})$ variations in $S_1(t)$. Hence, the pendulumlike picture has a time-dependent separatrix sweeping a narrow domain of size $O(N^{-1/2})$ around its average value. These fluctuations may cause particles to switch between trapped and untrapped motions. In this process, total momentum is conserved, so that

$$\frac{d}{dt}\sum_{r\in\text{TP}}\bar{p}_r=\frac{d}{dt}(N_{\text{TP}}\dot{\phi}_1)=-\frac{d}{dt}\sum_{r\in\text{UP}}\bar{p}_r,\qquad(14)$$

where N_{TP} is the number of trapped particles. Equation (14) shows that the drift velocity $\dot{\phi}_1$ changes mainly when a trapped particle becomes untrapped or the converse. Thus its time evolution is due to the small population of particles that evolve in the domain swept by the separatrix [3]. The change in the velocity of the particle with respect to the ''resonance'' [35–37] is proportional to the fluctuation of $S_1(t)$,

which is $O(N^{-1/2})$. The number of particles in the domain swept by the fluctuating separatrix (dN_{TP}/dt) scales also like $NN^{-1/2} \sim N^{1/2}$.

The global effect of these scalings is that the rate of change of the mean field $S_1(t)$ on the average scales as $N^{-1/2}N^{-1/2} = N^{-1}$. This rate of change is indeed the rate of decay of the amplitude $S_1(t)$.

Finally note that the trapping of a particle reduces S_1 while a detrapping enhances S_1. Indeed, a trapped particle at $x_r \approx \phi_1$ lies in a well generated by particles that repel it, so that particles responsible for the well lie near $\phi_1 + \pi$. Thus the particles generating the well are untrapped (they lie near the saddle of the resonance) and must move a little with respect to the resonance. The resonance can, however, subsist over a long time (with a small size: in our simulations $S_1 \approx 10^{-2}$) because particles near the saddle are slower than particles with the same e_r passing near the spatial center ϕ_1.

Let us stress that, as seen on Fig. 9, the resonance encloses a depletion of particles rather than an excess of particles. The argument above also explains why the turbulent structures of Sec. V are holes. Indeed, an excess of particles generates locally a saddle point, which repels the particles and destroys the cluster, whereas a depletion can be filled only by the (slower) trapping process described. This asymmetry between excess and depletions was already discussed in the plasma kinetic theory of clumps (see Ref. [16] and references therein). For the rotator model, neither long-lived density excess nor holes were generated when injecting a beam of particles in the system at velocities at which we remove the ''strips.''

C. Case $s > 1$

When the structures are present, $k_1V_1S_1 \gg k_nV_nS_n$ ($n \neq 1$), and $\phi_1(t)$ is slowly varying compared to $\phi_n(t)$, $3 \leq n \leq s'$. Consequently, the components of the force with $n \geq 3$ have small average effect and the dynamics is dominated by the first component S_1. However, the presence of the higher-order modes changes the shape of the ''resonance.'' As a first approximation, one may estimate that they enlarge the domain around the ''moving separatrix'' in which the particles get trapped or detrapped. Thus the characteristic time τ_v/N must decrease when s increases.

VII. INTERACTION OF HOLES

Finally, we turn to the interactions between (x,v)-space density holes and their dependence on initial conditions. These phenomena will be illustrated with the rotator ($s = 1$) model.

We consider initial distributions of $N = 20\,000$ particles with no spatial modulation and $L = 10\lambda_D$. The velocity distribution is a Maxwell distribution, from which we remove two strips $u - 0.025v_{th} \leq |v| \leq u + 0.025v_{th}$. The central velocity u takes values $0.15v_{th}$ and $0.25v_{th}$, significantly larger than the value $u = 0.055v_{th}$ used in the previous sections. The runs reveal the following qualitatively different evolutions.

For $u = 0.15v_{th}$, two holes appear in the velocity ranges $v \approx \pm u$, with sizes similar to the single hole of Sec. V B. They last until $t \approx 10^3 \omega_{pl}^{-1}$: at this time, the (x,v)-space density has reached equilibrium. These holes remain close to
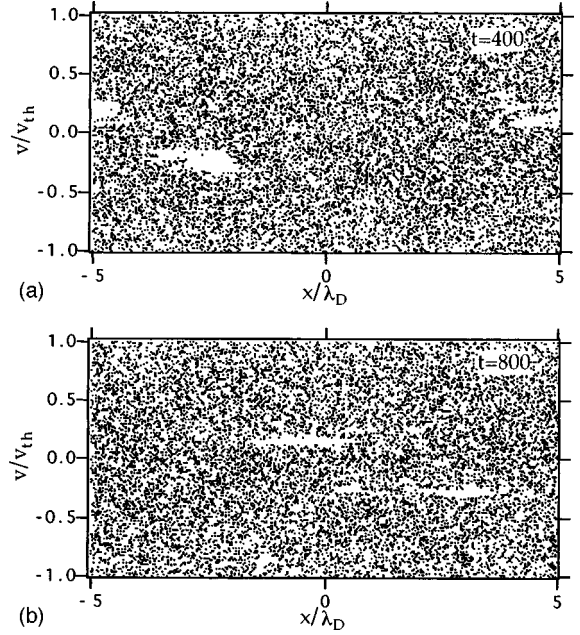

FIG. 14. (x,v) distribution of $N = 20\,000$ particles (with $L = 10\lambda_D$) in two-hole states at time t. Initial conditions have no spatial modulation and have a Maxwell distribution with two gaps $-0.025v_{th} \leq |v| - u \leq 0.025v_{th}$: (a) $u = 0.15v_{th}$, $t = 400\omega^{-1}$; (b) $u = 0.25v_{th}$, $t = 800\omega^{-1}$.

each other, forming a dipolelike structure as displayed on Fig. 14(a) at $t = 400\omega_{pl}^{-1}$.

For $u = 0.25v_{th}$, two holes appear similarly with velocities $\approx \pm u$ and with sizes similar to the previous ones. They last beyond $t = 2.10^3 \omega_{pl}^{-1}$. These holes [shown on Fig. 14(b) at $t = 800\omega_{pl}^{-1}$] move with respect to each other. In the process of their formation, smaller holes appear transiently and are absorbed by these two big ones.

Similar processes of hole formation and merging are known to occur and were observed in the kinetic theory of clumps in plasmas [13,17,39]. Our observations confirm the dynamical role of the holes in smooth interactions. In particular, we note that initial conditions with a ''missing strip'' in the velocity distribution function tend to generate a hole at the strip velocity. If one starts with two strips, two holes form, but they merge if their relative velocity is close to their characteristic width in v. On the contrary, if their relative velocity is significantly larger than their size in v, they behave rather independently [5].

The resonance description of Sec. VI B explains these various behaviors. First recall that, if a particle has a large velocity w relative to a resonance, the force acted by this resonance on the particle is averaged over a short time scale (L/w). Then, if two holes are present with very different phase velocities ($d\phi_{h1}/dt$, $d\phi_{h2}/dt$), one distinguishes three classes of particles: N_{h1} particles with velocity in the range of ''hole 1'' (i.e., with $|v - d\phi_{h1}/dt| \leq 2\sqrt{K'S_{h1}}$), similarly N_{h2} particles with velocity in the range of ''hole 2'' ($|v - d\phi_{h2}/dt| \leq 2\sqrt{K'S_{h2}}$), and $N_b = N - N_{h1} - N_{h2}$ ''background'' particles. In this classification, S_{h1} and S_{h2} are defined by the sum (4) restricted to the particles with velocity in their own range (to first approximation), which makes the definition of each class of particles self-consistent.

Denote by $\mathcal{S}_{\text{Chir}} := (2\sqrt{K'S_{h1}} + 2\sqrt{K'S_{h2}})/|d\phi_{h2}/dt - d\phi_{h1}/dt|$ the Chirikov overlap parameter of the resonances [40]. Then the total field $\mathbf{S}_1$ rewrites in the form $\mathbf{S}_1 = \mathbf{S}_{h1} + \mathbf{S}_{h2} + \mathbf{S}_b$, and the effective Hamiltonian generating the motion of a particle takes the paradigmatic two-resonance form $p_r^2/2 + K'S_{h1}\cos(x_r - \phi_{h1}) + K'S_{h2}\cos(x_r - \phi_{h2})$, neglecting $\mathbf{S}_b$. For the latter Hamiltonian [40], if the two resonances do not overlap (i.e., if $\mathcal{S}_{\text{Chir}} < 1$), the particle motion is rather regular: it is trapped in one of the resonances or it moves quite freely. But if the two resonances overlap ($\mathcal{S}_{\text{Chir}} \gtrsim 1$), a particle that should be trapped in one of the resonances moves chaotically from one resonance to the other (and incidentally our definition of the two classes ''h1'' and ''h2'' breaks down). As the motion of holes is just the same as the motion of test particles, this implies that holes can keep their identities over a significant time scale only if their relative velocity is large enough [41].

Practically, the Chirikov resonance overlap parameter may be grossly estimated as follows. The relative phase velocity $|d\phi_{h2}/dt - d\phi_{h1}/dt| \approx 2u$ is checked directly from the figures. The half-width of each resonance is estimated from the aspect ratio of its hole: the hole has a characteristic length Δx ($\approx \lambda_D$) and a characteristic width in velocity Δv ($\approx 0.1 v_{\text{th}}$). The ratio $\Delta v/\Delta x$ is the bounce frequency ω_{trap} at the bottom of the resonance's potential well (provided $\Delta x \ll L$ for a period-L cosine potential), and the resonance half-width is thus $(L/\pi)\Delta v/\Delta x$. For the cases displayed on the figures, $\omega_{\text{trap}} \approx 0.1\omega_{\text{pl}}$ yields the estimates $\mathcal{S}_{\text{Chir}} = 0.2 v_{\text{th}}/(2u)$, which is smaller than 1 for Figs. 14(a) and 14(b). However, for the initial data with $u = 0.055 v_{\text{th}}$, a similar estimate would yield $\mathcal{S}_{\text{Chir}} \gtrsim 1$, implying that the holes should merge, as they do indeed.

VIII. CONCLUSIONS

To summarize, given initial conditions out of equilibrium, we have shown that the systems in our family generate turbulent structures analogous to those studied with the kinetic plasma models [16]. The existence of these structures and their lifetime are dominated by spatial scales larger than the Debye length λ_D. The relaxation time to thermal equilibrium is not strongly affected by the turbulence. This suggests that the phase space, or (x,v) space, mixing due to the tur-

bulent structures may be small. Indeed the dominant process for the evolution of the structures is separatrix crossing in (x,v) space, i.e., trapping-detrapping of particles in the resonance associated with the long wavelength field component. This process is sensitive to the particle number density: Its characteristic time scale is proportional to N (or to $N_D = N\lambda_D/L$) although the macroscopic time scale ω_{pl} is independent of N.

Our results also show that important dynamical properties of the 1D Coulombian system are well reproduced, even quantitatively, by the dynamics of the rotator model (2), which is easily simulated numerically by molecular dynamics. This validates the use of direct molecular dynamics (possibly with truncation to Fourier components with scales larger than λ_D, in a kind of spectral code) as an alternative to kinetic-theory based codes for electrostatic plasma turbulence, such as classical particle-in-cell codes. Besides, our observation of holes for finite s and finite N shows that their formation is not related to the ability of the Vlasov-Poisson system to generate singularities [23].

This work leaves open several interesting problems. The first is to discuss similarly the evolution of structures in attractive potentials, such as the gravitational one and the ferromagnetic XY model [42–44,3,12]. The second is the low temperature dynamics for repulsive models, as long-lived clusters have been observed in the $s = 1$ rotator model [3]. The third is the interaction of the turbulent structures considered here with large perturbations of hydrodynamic type. This will be the subject of forthcoming works.

[1] R. Balescu, *Statistical Mechanics of Charged Particles* (Interscience, New York, 1963).
[2] M. Baus and J. P. Hansen, Phys. Rep. **59**, 1 (1979).
[3] M. Antoni and S. Ruffo, Phys. Rev. E **52**, 2361 (1995).
[4] M. Antoni, C. Sandoz, and Y. Elskens, in *Hamiltonian Systems with Three or More Degrees of Freedom*, edited by C. Simó (Kluwer, Dordrecht, in press).
[5] C. Sandoz, Thèse de doctorat de l'université de Provence, Marseille, 1995 (unpublished).
[6] C. Sandoz, M. Antoni, and Y. Elskens, in *Transport, Chaos and Plasma Physics 2,* edited by S. Benkadda, F. Doveil, and Y. Elskens (World Scientific, Singapore, 1996), pp. 105–110.
[7] M. Antoni, Thèse de doctorat de l'université de Provence, Marseille, 1993 (unpublished).
[8] M. Antoni and D. F. Escande, in *Transport, Chaos and Plasma Physics*, edited by S. Benkadda, F. Doveil, and Y. Elskens (World Scientific, Singapore, 1994), pp. 120–123.
[9] M. Antoni, Y. Elskens, and D. F. Escande, in *Dynamics of Transport in Plasmas and for Charged Beams*, edited by G. Maino and M. Ottaviani (World Scientific, Singapore, 1996), pp. 1–17.
[10] M. Antoni, Y. Elskens, and D. F. Escande, Phys. Plasmas (to be published).
[11] V. Latora, A. Rapisarda, and S. Ruffo, Phys. Rev. Lett. **80**, 692 (1998).
[12] S. Ruffo, in *Transport, Chaos and Plasma Physics*, edited by S. Benkadda, F. Doveil, and Y. Elskens (World Scientific, Singapore, 1994), pp. 114–119.

[13] H. L. Berk, C. E. Nielsen, and K. V. Roberts, Phys. Fluids **13**, 980 (1970).

[14] T. Boutros-Ghali and T. H. Dupree, Phys. Fluids **24**, 1839 (1981).

[15] T. H. Dupree, Phys. Fluids **25**, 277 (1982).

[16] R. H. Berman, D. J. Tetreault, and T. H. Dupree, Phys. Fluids **26**, 2437 (1983).

[17] A. Ghizzo, B. Izrar, P. Bertrand, E. Fijalkow, M. R. Feix, and M. Shoucri, Phys. Fluids **31**, 72 (1988).

[18] H. Schamel, Phys. Rep. **140**, 161 (1986).

[19] J. H. Misguich and R. Balescu (unpublished).

[20] H. Schamel and J. Korn, Phys. Scr. **T63**, 63 (1996).

[21] H. Neunzert, in *Kinetic Theories and the Boltzmann Equation*, edited by C. Cercignani, Lecture Notes in Mathematics No. 1048 (Springer, Berlin, 1984), pp. 60–110.

[22] H. Spohn, *Large Scale Dynamics of Interacting Particles* (Springer, Berlin, 1991).

[23] A. J. Majda, G. Majda, and Y. Zheng, Physica D **74**, 268 (1994).

[24] Y. Elskens and M. Antoni, Phys. Rev. E **55**, 6575 (1997).

[25] A. Lenard, J. Math. Phys. **2**, 682 (1961).

[26] S. Prager, in *Advances in Chemical Physics*, edited by I. Prigogine (Wiley-Interscience, New York, 1962), Vol. 4, pp. 201–224.

[27] B. B. Kadomtsev, *Plasma Turbulence* (Academic, London, 1965) (translated by L. C. Ronson and M. C. Rusbridge).

[28] V. Latora, A. Rapisarda, and S. Ruffo, Ref. 23 in [11].

[29] J. R. Cary and I. Doxas, J. Comput. Phys. **107**, 98 (1993).

[30] O. C. Eldridge and M. Feix, Phys. Fluids **5**, 1076 (1962).

[31] M. R. Feix, in *Nonlinear Effects in Plasmas*, edited by G. Kalman and M. Feix (Gordon and Breach, New York, 1969), pp. 151–196.

[32] J. L. Rouet, Thèse de doctorat de l'université d'Orléans, Orléans, 1990 (unpublished).

[33] J. L. Rouet and M. R. Feix, Phys. Fluids B **3**, 1830 (1991).

[34] E. M. Lifshitz and L. P. Pitaevskii, *Physical Kinetics* (Pergamon, Oxford, 1981) (translated by J. B. Sykes and R. N. Franklin).

[35] J. R. Cary, D. F. Escande, and J. L. Tennyson, Phys. Rev. A **34**, 4256 (1986).

[36] Y. Elskens and D. F. Escande, Nonlinearity **4**, 615 (1991).

[37] Y. Elskens and D. F. Escande, Physica D **62**, 66 (1992).

[38] I. B. Bernstein, J. M. Greene, and M. D. Kruskal, Phys. Rev. **108**, 546 (1957).

[39] A. Ghizzo, B. Izrar, P. Bertrand, M. R. Feix, E. Fijalkow, and M. Shoucri, Phys. Lett. A **120**, 191 (1987).

[40] D. F. Escande, Phys. Rep. **121**, 165 (1985).

[41] Similarly, resonance considerations enable one to associate Langmuir modes with components of the field propagating with phase velocities much larger than the thermal velocity [10].

[42] Ch. J. Reidl and B. N. Miller, Phys. Rev. E **51**, 884 (1995).

[43] T. Tsuchiya, N. Gouda, and T. Konishi, Phys. Rev. E **53**, 2210 (1996).

[44] S. Inagaki, Prog. Theor. Phys. **90**, 577 (1993); S. Inagaki and T. Konishi, Publ. Astron. Soc. Jpn. **45**, 733 (1993).